

Photosensitizing Hollow Nanocapsules for Combination Cancer Therapy**

Kyung Jin Son, Hee-Jae Yoon, Joo-Ho Kim, Woo-Dong Jang,* Yeol Lee, and Won-Gun Koh*

The social and economic burden of cancer demands a spectrum of therapeutic methodologies. Current options include surgery, chemotherapy, radiotherapy, hyperthermia,^[1] and photodynamic therapy (PDT).^[2] Only rarely, however, is a single methodology sufficient to overcome cancer. This requirement has inspired combination regimens that overcome the additive, synergistic, and complementary interactions between treatments.^[3] An important advance in combination cancer therapy was achieved with the fabrication of multifunctional nanomaterials, including polymeric micelles and nanoparticles (NPs), which may be used to simultaneously perform more than one therapy.^[4]

Polymeric multilayer capsules present several advantages in combination cancer therapy, including a relatively high capacity for the active substance and versatility in fabrication of the capsule shell.^[5] The hollow capsules are assembled in a layer-by-layer (LbL) process onto a sacrificial template followed by dissolution of the template.^[6] Hollow polymeric capsules can be fabricated by using templates that vary in size from a few nanometers to hundreds of micrometers, and their chemical and mechanical properties can be precisely tailored by modulating the thickness and composition of the shell.^[7] Polymeric multilayer capsules attract interest in various fields of research, and most recently for their high loading capacity as vehicles in drug delivery systems (DDSs).^[8]

Based on this background, we developed a new type of hollow nanocapsule (NC) for use in combining PDT with chemotherapy. To produce the photosensitizer, we synthesized a negatively charged dendritic porphyrin (DP) that was shown to be effective photosensitizer for PDT,^[9] and combined it as a bilayer component with poly(allylamine hydro-

chloride) (PAH) to fabricate hollow NCs. In general, photosensitizers have large π -conjugation domains for high quantum yields and effective energy absorption. Therefore, many photosensitizers can easily form aggregates in aqueous media because of their abilities to form π - π interactions and their hydrophobic characteristics, which provide a self-quenching effect of the excited state. Unlike conventional photosensitizers, DP has large dendritic wedges that effectively prevent self-quenching phenomena. Moreover, when the DP forms self-assembled nanostructures such as polymeric micelles, large numbers of DPs can effectively generate a high concentration of singlet oxygen at local sites in order to overcome the threshold concentration for oxidative damage.

The (PAH/DP)_n multilayer nanocapsules were filled with doxorubicin (DOX), a model anticancer drug, in order to implement chemotherapy. While most NC shells used in DDS are prepared from linear polyelectrolytes that lack any function other than drug container, our system employs DP as not only a polyelectrolyte for the formation of NC shells but also as photosensitizing units for photodynamic therapy.

Figure 1 shows the preparation of hollow NCs by alternating deposition of PAH and DP onto a negatively charged polystyrene (PS) NP and the subsequent removal of the template PS NP. The average molecular weight of PS was determined to be 70 kDa by GPC analysis. It has been reported that dissolved PS ($M_w \approx 10^6$ Da) can diffuse through the multilayer shells when they were extracted with organic solvents such as chloroform or tetrahydrofuran.^[10] The DP used in this study bears 32 carboxylate groups on its periphery and a negative zeta potential (−31.0 mV) at pH 7.4. We expected that multilayer shells would be formed by this LbL deposition technique based on the electrostatic interaction between positively charged PAH and negatively charged DP. The stepwise formation of multilayer shells onto PS NPs was monitored by observing zeta potential changes of particles after each deposition step (Figure 2a). The bare PS NPs have a zeta potential of approximately −55 mV. The PS NPs coated with layers of PAH and DP showed discrete zeta potentials that alternate between positive or negative, depending on the outer layer type. This observation showed that the multilayer surface was charge-overcompensated in each adsorption step, which facilitated adsorption of the next oppositely charged capsule shell layer. Owing to the strong UV/Vis absorbance and fluorescence (FL) emission of DP, multilayer formation could be monitored by changes in UV/Vis absorbance and FL emission from the multilayer-coated PS particles (NC_n/PS; n = numbers of LbL bilayer, n = 1–3). As shown in Figure 2b, the UV/Vis absorbance and FL emission increased with the number of bilayers. Quantities of DP deposited in NCs were determined to be (106.2 ± 0.4) , (212.6 ± 0.4) , and $(366.1 \pm$

[*] K. J. Son,^[†] Y. Lee, Prof. W.-G. Koh
Department of Chemical and Biomolecular Engineering
Yonsei University
50 Yonsei-ro, Seodaemun-Gu, Seoul 120-749 (Korea)
E-mail: wongun@yonsei.ac.kr

H.-J. Yoon,^[†] J.-H. Kim, Prof. W.-D. Jang
Department of Chemistry, Yonsei University
50 Yonsei-ro, Seodaemun-Gu, Seoul 120-749 (Korea)
E-mail: wdjang@yonsei.ac.kr

[†] These authors contributed equally to this work.

[**] This work was supported by the National Research Foundation (NRF) grant funded by the Korean government (R11-2007-050-03002-0: Active Polymer Center for Pattern Integration, 2011-0001126: Center for Bioactive Molecular Hybrids, and 20100019175) and the KRIBB Research Initiative Program. K.J.S., H.-J.Y., J.K., and Y.L. acknowledge fellowships from the BK21 program from MEST, Korea.



Supporting information for this article is available on the WWW under <http://dx.doi.org/10.1002/anie.201102658>.

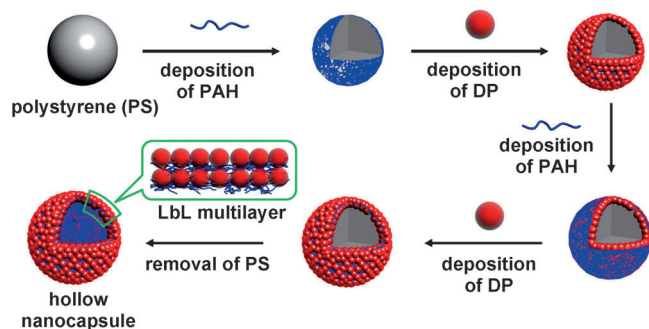
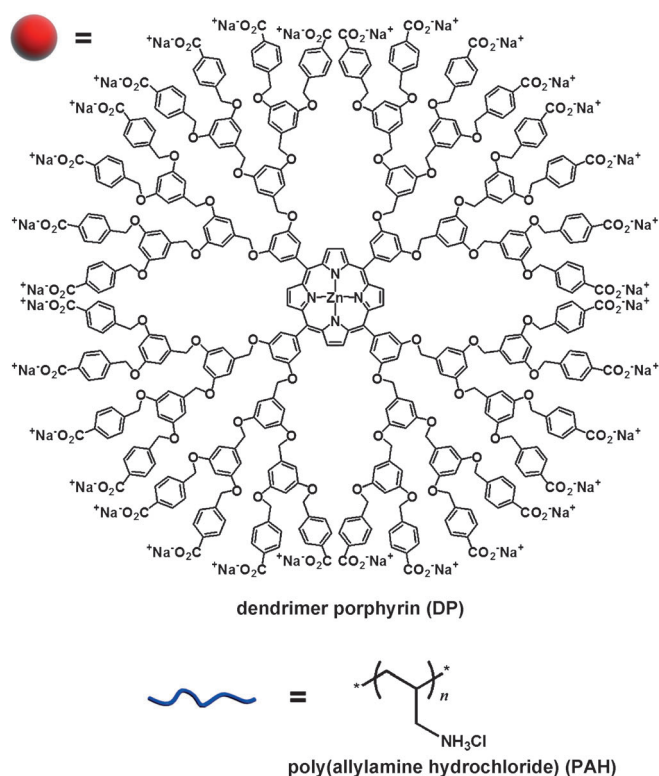


Figure 1. Procedure for the preparation of multilayer hollow nanocapsules.

0.9) $\mu\text{g mg}^{-1}$ of PS particles for NC₁, NC₂, and NC₃, respectively. Thus the DP content of the NCs, and hence the strength of the PDT effect, could be easily controlled by adjusting the number of layers deposited.

TEM and FE-SEM studies (Figure 3a) showed the formation of multilayered hollow NCs and the creased morphology of these NCs, in contrast to the smooth NCs \supset PS. However, even one bilayer was sufficiently stable and maintained its globular shape after removing the template PS NP. TEM images of hollow NCs also showed a higher degree of electron transmission than NCs \supset PS. FE-SEM showed that the creases became fewer and deeper as the number of bilayers increased, which may result from the differences in thickness between shells. To investigate their stability, NCs were treated with solutions of various pH values for 1 day, and then observed by FE-SEM. The NCs retained their shape even when kept under strongly acid (pH 3) or basic (pH 11) conditions (Figure 3b).

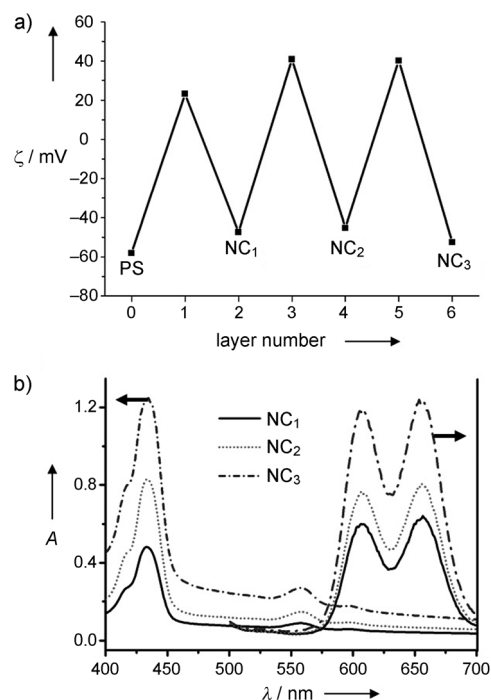


Figure 2. Formation of multilayers on PS nanoparticles. a) Changes in zeta potential by the number of PAH or DP layers deposited, b) UV/Vis absorption and fluorescence emission spectra of NC_n ($n = 1, 2, 3$).

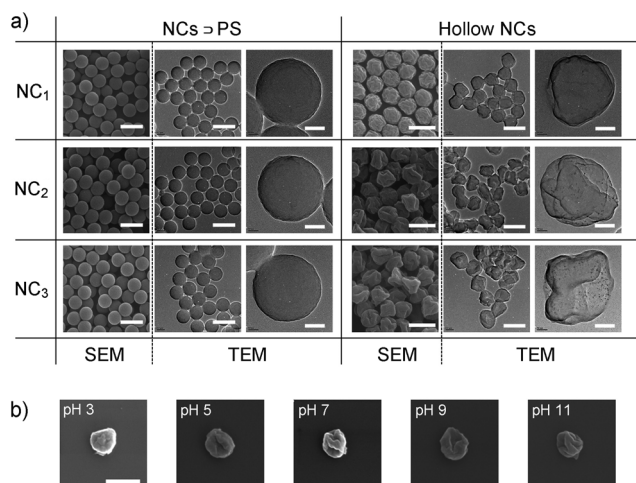


Figure 3. SEM and TEM images of NCs. a) SEM and TEM images of NCs before and after removal of PS nanoparticles. b) SEM images of hollow nanocapsules (NC₃) that were treated with solutions of different pH values for 1 day. Scale bars 500 nm except for right-hand TEM images (100 nm).

Because the NCs were stable and have a large inner cavity, we tested these compounds for drug delivery by loading them with doxorubicin hydrochloride (DOX) as this drug is water-soluble and has been frequently used in multilayer capsules.^[8b,11] Loading of this model anticancer drug into DP-containing capsules should produce NCs with both PDT and chemotherapeutic capability. Both NCs and NCs \supset PS were incubated with a solution of DOX (800 $\mu\text{g mL}^{-1}$ in PBS) for 24 h followed by centrifugation and washing, in order to load

DOX into the NCs. The loading amount as a function of time was estimated by the UV/Vis absorption at 480 nm (Figure 4a). NCs \supset PS contained only very small amounts of DOX because the drug could only adsorb onto the multilayer shells. The hollow NCs could be loaded with significantly greater

of free amino groups in non-cross-linked NCs. The EDC/NHS cross-linking reaction significantly decreased the free amine concentration and that the degree of cross-linking was dependent on reaction time. The release of DOX from NCs \supset DOX was dependent on the degree of cross-linking. For

example, if the cross-linking reaction continued for more than 2 h, the capsule shells became impermeable to DOX, and did not allow release of the drug. However, by controlling the degree of cross-linking, we could achieve sustained release of DOX from NCs \supset DOX for a much longer time than from non-cross-linked NCs \supset DOX; for example, NCs \supset DOX that were cross-linked for 30 min continued to release DOX for more than 4 days (Figure 4b; cross-linked NCs). Although a single-bilayer capsule released slightly more DOX than the others for the initial 24 h, the release behavior was essentially independent of the number of bilayers (up to three bilayers), as was loading.

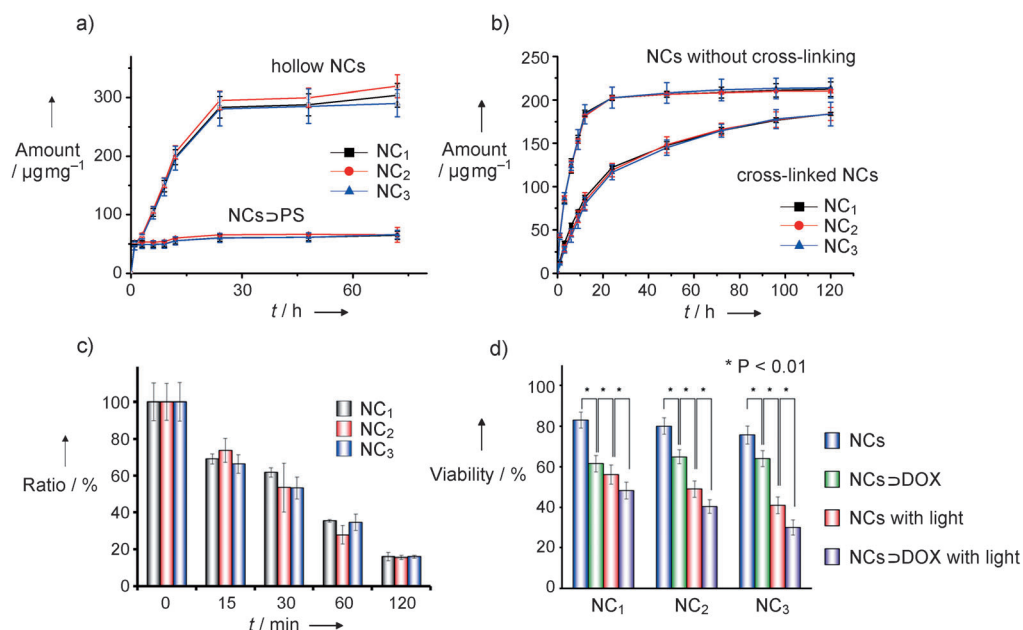


Figure 4. Characteristics of NCs. a) Amount of DOX loading in hollow NCs and NCs \supset PS. b) Amount of DOX released from cross-linked and non-cross-linked NCs. c) Relationship between reaction time of EDC/NHS cross-linking on the percentage of free amine content of multilayer shells in NCs. (d) Comparison of cell viability following chemotherapy (NCs \supset DOX), photodynamic therapy (NCs with light), and combined therapy (NCs \supset DOX with light).

quantities of DOX, thus indicating that DOX could diffuse easily through the LbL membrane and fill the hollow NCs. The number of bilayers (1, 2, and 3) did not significantly influence the loading rate or total amount of loaded DOX. The amount of DOX loaded into the hollow NCs increased linearly with incubation time and reached a maximum value after 24 h. The difference in DOX-loading capacity between NCs \supset PS and NCs is another indication that the PS particles were successfully removed to produce the multilayer hollow NCs. After successful DOX loading, the release behavior of hollow capsules was studied by the incubation of NCs \supset DOX in phosphate-buffered saline (PBS). Because DOX was loaded into NCs without altering any property of the multilayer shell, the release profile resembled the loading profile of DOX (Figure 4b; NCs without cross-linking), that is, the release rate was very rapid and largely complete within 24 h. To control the release rate, the shells were cross-linked using *N*-hydroxysuccinimide (NHS) and 1-ethyl-3-(3-dimethylaminopropyl) carbodiimide (EDC). Because the carboxylic acid moieties in DP and amino groups in PAH were already in proximity and form a stable ionic complex, treatment with EDC/NHS generated stable amide bonds. The degree of cross-linking was monitored by a ninhydrin assay.^[12] Figure 4c shows the change of free amino groups in NCs with cross-linking time, where the values are normalized by the amount

The effective use of DP as a photosensitizer in PDT is well-documented.^[13] This activity stems from photoexcitation of a porphyrin, which then generates reactive oxygen species (ROS) by energy transfer or electron transfer to oxygen molecules.^[14] In this study, we have incorporated DP into the NCs to be used as a drug delivery system, in order to combine PDT with chemotherapy. The sustained DOX release and ROS generation by photoirradiation may thus be applied simultaneously to treat a malignant tumor. To evaluate the feasibility of this combination cancer therapy, HeLa cells (4000 cells per well) were incubated with NCs or NCs \supset DOX in 48-well culture plates for 48 h ($n = 12$), where the amount of encapsulated DOX was fixed at $50 \mu\text{g mL}^{-1}$ for all NCs \supset DOX. The DP concentrations of NC₁, NC₂, and NC₃ were estimated to be 0.76, 1.5, and 2.6 nm, respectively. The culture medium was then exchanged to remove all the NCs that were not taken up by cells and further incubated for 24 h to ensure sufficient DOX release. Photoirradiation was applied for 1 h with a broad-band visible light from a light-emitting diode (LED; incident energy 132 kJ cm^{-2}). Figure 4d shows the viability of HeLa cells after chemotherapy alone, PDT alone, and combined therapy at the optimum concentration ($31.3 \mu\text{g mL}^{-1}$ of NCs) for the optimum visualization of both effects. At this concentration, without DOX release and photoirradiation, cell viability was approximately 80% for all

NC treatments. The viability decreased to about 60% when the cells were incubated with NCs/DOX without photoirradiation because of the effect of DOX. When photoirradiation alone was applied using DOX-free NCs, the NCs induced strong photocytotoxicity. Such strong photocytotoxicity was not observable in the treatment of free DP. The NC₃ exerted the strongest effect because they contained the largest amount of DP in the capsule wall, which is further supported by the IC₅₀ values of hollow NCs based on the concentration of DP. The IC₅₀ values are dependent of the number of layers, whereas the cytotoxicity cannot be directly correlated to the concentration of photosensitizers because the photocytotoxicity is not directly originated from photosensitizers but from reactive oxygen species generated by photoirradiation to photosensitizers.^[15] When the NCs/DOX were irradiated, all systems showed higher cytotoxicity than with either chemotherapy or PDT alone; this effect thus results from the combination of chemotherapy and PDT.

In summary, we fabricated DOX-loaded PAH/DP multilayer NCs that may potentially deliver combined cancer therapy. DP, which is a component in the LbL assembly of the NC shell, served as a photosensitizing agent for PDT, and the amount of DP was controlled by changing the number of layers deposited. DOX easily permeated the multilayer shells and filled the hollow NCs; subsequent cross-linking between PAH and DP allowed controlled release of DOX from the hollow NCs. Cell viability studies showed that combined treatment resulted in higher toxicity than either chemotherapy or PDT alone.

Received: April 18, 2011

Revised: July 8, 2011

Published online: October 17, 2011

Keywords: antitumor agents · dendrimers · nanoparticles · photodynamic therapy · porphyrinoids

- [1] M. H. Falk, R. D. Issels, *Int. J. Hyperthermia* **2001**, *17*, 1–18.
- [2] a) D. E. J. G. J. Dolmans, D. Fukumura, R. K. Jain, *Nat. Rev. Cancer* **2003**, *3*, 380–387; b) T. J. Dougherty, C. J. Gomer, B. W. Henderson, G. Jori, D. Kessel, M. Korbek, J. Moan, Q. Peng, *J. Natl. Cancer Inst.* **1998**, *90*, 889–905; c) R. Bonnett, *Chemical Aspects of Photodynamic Therapy*, Gordon and Breach, Amsterdam, **2000**; d) E. C. Korngold, J. R. McCarthy, J. L. Figueiredo, E. Aikawa, R. H. Kohler, R. Weissleder, F. A. Jaffer, *Circulation* **2007**, *116*, 241–241; e) R. K. Pandey, G. Zheng, *The Porphyrin Handbook*, Vol. 6, Academic Press, San Diego, **2000**; f) H. He, P.-C. Lo, S.-L. Yeung, W.-P. Fong, D. K. P. Ng, *Chem. Commun.* **2011**, *47*, 4748–4750; g) X. J. Jiang, P. C. Lo, Y. M. Tsang, S. L. Yeung, W. P. Fong, D. K. P. Ng, *Chem. Eur. J.* **2010**, *16*, 4777–4783.
- [3] a) J. A. Green, J. M. Kirwan, J. F. Tierney, P. Symonds, L. Fresco, M. Collingwood, C. J. Williams, *Lancet* **2001**, *358*, 781–786; b) H. J. Mauceri, N. N. Hanna, M. A. Beckett, D. H. Gorski, M. J. Staba, K. A. Stellato, K. Bigelow, R. Heimann, S. Gately, M. Dhanabal, G. A. Soff, V. P. Sukhatme, D. W. Kufe, R. R. Weichselbaum, *Nature* **1998**, *394*, 287–291; c) F. Y. Cheng, C. H. Su, P. C. Wu, C. S. Yeh, *Chem. Commun.* **2010**, *46*, 3167–3169; d) A. Khadair, D. Chen, Y. Patil, L. Ma, Q. P. Dou, M. P. Shekhar, J. Panyam, *J. Controlled Release* **2010**, *141*, 137–144; e) C. M. Peterson, J. M. Lu, Y. Sun, C. A. Peterson, J. G. Shiah, R. C. Straight, J. Kopecek, *Cancer Res.* **1996**, *56*, 3980–3985; f) J. G. Shiah, Y. Sun, P. Kopeckova, C. M. Peterson, R. C. Straight, J. Kopecek, *J. Controlled Release* **2001**, *74*, 249–253; g) M. J. Shieh, C. L. Peng, P. S. Lai, F. H. Lin, S. Y. H. Wu, *Biomaterials* **2009**, *30*, 3614–3625; h) K. H. Yoo, H. Park, J. Yang, J. Lee, S. Haam, I. H. Choi, *ACS Nano* **2009**, *3*, 2919–2926.
- [4] a) J. Kim, H. J. Yoon, S. Kim, K. Wang, T. Ishii, Y. R. Kim, W. D. Jang, *J. Mater. Chem.* **2009**, *19*, 4627–4631; b) L. Brannon-Peppas, J. O. Blanchette, *Adv. Drug Delivery Rev.* **2004**, *56*, 1649–1659; c) I. Brigger, C. Dubernet, P. Couvreur, *Adv. Drug Delivery Rev.* **2002**, *54*, 631–651; d) R. Misra, S. Acharya, S. K. Sahoo, *Drug Discovery Today* **2010**, *15*, 842–850; e) J. H. Park, S. Lee, J. H. Kim, K. Park, K. Kim, I. C. Kwon, *Prog. Polym. Sci.* **2008**, *33*, 113–137; f) D. Peer, J. M. Karp, S. Hong, O. C. Farokhzad, R. Margalit, R. Langer, *Nat. Nanotechnol.* **2007**, *2*, 751–760; g) J. F. Lovell, C. S. Jin, E. Huynh, H. L. Jin, C. Kim, J. L. Rubinstein, W. C. W. Chan, W. G. Cao, L. V. Wang, G. Zheng, *Nat. Mater.* **2011**, *10*, 324–332; h) K. Kim, J. H. Kim, H. Park, Y. S. Kim, K. Park, H. Nam, S. Lee, J. H. Park, R. W. Park, I. S. Kim, K. Choi, S. Y. Kim, K. Park, I. C. Kwon, *J. Controlled Release* **2010**, *146*, 219–227; i) W. F. Dong, A. Kishimura, Y. Anraku, S. Chuano, K. Kataoka, *J. Am. Chem. Soc.* **2009**, *131*, 3804–3805.
- [5] X. Y. Liu, C. Y. Gao, J. C. Shen, H. Mohwald, *Macromol. Biosci.* **2005**, *5*, 1209–1219.
- [6] a) L. J. De Cock, S. De Koker, B. G. De Geest, J. Grooten, C. Vervaeke, J. P. Remon, G. B. Sukhorukov, M. N. Antipina, *Angew. Chem.* **2010**, *122*, 7108–7127; *Angew. Chem. Int. Ed.* **2010**, *49*, 6954–6973; b) M. Delcea, A. Yashchenok, K. Videnova, O. Kreft, H. Mohwald, A. G. Skirtach, *Macromol. Biosci.* **2010**, *10*, 465–474.
- [7] a) G. Decher, *Science* **1997**, *277*, 1232–1237; b) Y. Wang, A. S. Angelatos, F. Caruso, *Chem. Mater.* **2008**, *20*, 848–858.
- [8] a) A. P. R. Johnston, C. Cortez, A. S. Angelatos, F. Caruso, *Curr. Opin. Colloid Interface Sci.* **2006**, *11*, 203–209; b) A. J. Khopade, F. Caruso, *Biomacromolecules* **2002**, *3*, 1154–1162.
- [9] a) W.-D. Jang, N. Nishiyama, G. D. Zhang, A. Harada, D. L. Jiang, S. Kawauchi, Y. Morimoto, M. Kikuchi, H. Koyama, T. Aida, K. Kataoka, *Angew. Chem.* **2005**, *117*, 423–427; *Angew. Chem. Int. Ed.* **2005**, *44*, 419–423; b) Y. Li, W.-D. Jang, N. Nishiyama, A. Kishimura, S. Kawauchi, Y. Morimoto, S. Mlake, T. Yamashita, M. Kikuchi, T. Aida, K. Kataoka, *Chem. Mater.* **2007**, *19*, 5557–5562.
- [10] a) M. Akashi, M. Matsusaki, *Expert Opin. Drug Delivery* **2009**, *6*, 1207–1217; b) F. Caruso, *Chem. Eur. J.* **2000**, *6*, 413–419; c) C. Dejngnat, G. B. Sukhorukov, *Langmuir* **2004**, *20*, 7265–7269; d) C. S. Peyratout, L. Dahne, *Angew. Chem.* **2004**, *116*, 3850–3872; *Angew. Chem. Int. Ed.* **2004**, *43*, 3762–3783.
- [11] X. Tao, H. Chen, X. J. Sun, H. F. Chen, W. H. Roa, *Int. J. Pharm.* **2007**, *336*, 376–381.
- [12] J. Ward, J. Kelly, W. X. Wang, D. I. Zeugolis, A. Pandit, *Biomacromolecules* **2010**, *11*, 3093–3101.
- [13] a) W.-D. Jang, Y. Nakagishi, N. Nishiyama, S. Kawauchi, Y. Morimoto, M. Kikuchi, K. Kataoka, *J. Controlled Release* **2006**, *113*, 73–79; b) N. Nishiyama, Arnida, W.-D. Jang, K. Date, K. Miyata, K. Kataoka, *J. Drug Targeting* **2006**, *14*, 413–424.
- [14] A. M. D. Battle, *J. Photochem. Photobiol. B* **1993**, *20*, 5–22.
- [15] a) R. Ideta, F. Tasaka, W.-D. Jang, N. Nishiyama, G. D. Zhang, A. Harada, Y. Yanagi, Y. Tamaki, T. Aida, K. Kataoka, *Nano Lett.* **2005**, *5*, 2426–2431; b) W.-D. Jang, N. Nishiyama, K. Kataoka, *Supramol. Chem.* **2007**, *19*, 309–314; c) K. Kataoka, W.-D. Jang, Y. Nakagishi, N. Nishiyama, S. Kawauchi, Y. Morimoto, M. Kikuchi, *J. Controlled Release* **2006**, *113*, 73–79; d) N. Nishiyama, Arnida, N. Kanayama, W.-D. Jang, Y. Yamasaki, K. Kataoka, *J. Controlled Release* **2006**, *115*, 208–215.